Six-Electron Organic Redoxmers for Aqueous Redox Flow Batteries

COMMUNICATION

Six-Electron Organic Redoxmers for Aqueous Redox Flow Batteries

Xiaoting Fang,[a,b,c] Andres T. Cavazos,[a] Zhiguang Li,[a,b,c] Chenzhao Li,[a,b] Jian Xie,[a] Stephen R. Wassall,[a] Lu Zhang,[c]* and Xiaoliang Wei [a]*

**We have developed a novel molecular design that enables six-electron redox activity in fused phenazine-based organic scaffolds. Combined electrochemical and spectroscopic tests successfully confirm the two-step 6e⁻ redox mechanism. This work offers an opportunity for achieving energy-dense redox flow batteries, on condition that the solubility and stability issues are addressed.**

The fast-growing deployment of clean, abundant renewable energies has raised concerns of grid reliability and energy security, because of their intermittent nature. To address this challenge, redox flow battery (RFB) has been introduced as a highly competitive stationary energy storage solution. Spatial decoupling of redox materials from the electrodes, rendering independent energy and power scalability especially when storage times longer than 4 hours are required.[1, 2] All-vanadium RFB is the best known system because of long cycle life, but the low energy density (~30 WhL⁻¹) and high vanadium cost are daunting barriers for widespread uptake.[3] Recently, organic redox molecules (or redoxmers) have attracted great interest, because of the remarkable advantages of structural diversity and chemical tailorability.[4, 5] A variety of organic redoxmers show encouraging property and performance sets in RFBs, but those of commercialization significance are still rather rare. The major drawbacks include low energy density and short cycle life, owing mainly to limited solubility and chemical stability, respectively.

Redoxmers with more than one transferred electrons are promising to achieve increased energy density. Many organic redoxmers exhibit 1e⁻ electrochemistry,[6, 7] and a few are capable of 2e⁻ reactions,[8] including quinone,[9, 10] phenazine,[11, 12] phenothiazine,[13] etc. Redoxmers with ≥3e⁻ reactions can lead to theoretically tripled energy density per unit of redoxmer, but remain a highly under-addressed area of research in RFB field,[14, 15] resulting in a missed opportunity critically important for further increasing energy density.

Here, we report a novel molecular design of organic macrocyclic anolyte redoxmers that are capable of 6e⁻ redox properties in aqueous RFBs. As shown in Scheme 1, the redoxmer molecules incorporate a tripod core of fused heteroaromatic rings to offer the 6e⁻ activity and the required chemical stability via charge delocalization. Our previous study has showed that a phenazine analog, 7,8-dihydroxyphenazine-2-sulfonic acid (**DHPS**), demonstrates remarkable solubility, stability and 2e⁻ redox in alkaline RFBs.[11] Inspired by this work, a fused tripod phenazine core (abbreviated as **TPz**) is used as the 6e⁻ redox center. To enable solubility in water, hydrophilic substituents are introduced to solubilize the macrocyclic moiety. In addition, the bulky molecular size of **TPz** helps minimize redoxmer crossover through the cation exchange membrane used in RFBs.
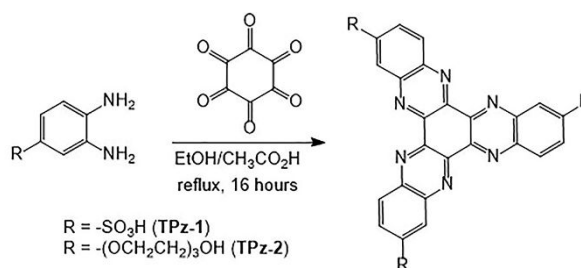
Scheme 1. Synthesis of **TPz** molecules.

A couple of **TPz** derivatives (**TPz-1** and **TPz-2**) were successfully synthesized via highly scalable coupling reactions between hexaketocyclohexane and structurally tailored *ortho*-diaminobenzene (Scheme 1). Typically, the reactant mixture was refluxed in a mixed solvent of ethanol and acetic acid (1:1 by volume) to obtain the title products in >80% purified yields. The *ortho*-diaminobenzene precursors that are not commercially available were synthesized in our lab. The detailed procedures of synthesizing **TPz-1** and **TPz-2** are described in Section S2 of the ESI. **TPz-1** bears three sulfonic acids as the solubilizing substituents, but the solubility is only 0.05 M in 1 M NaOH. Replacing the three sulfonic acids with tri(ethylene glycol) groups in **TPz-2** boosts the solubility to 0.3 M. Considering the 6e⁻ reaction, this is equivalent to 1.8 M of transferred electrons. Therefore, **TPz-2** was used to evaluate the performance in ensuing electrochemical and flow cell tests. The water-soluble parent phenazine, **DHPS**, was also synthesized and tested as the baseline case.

a. Indiana University-Purdue University Indianapolis, 425 University Boulevard, Indianapolis, IN 46202, USA. Email: xwei18@iupui.edu.
b. Purdue University, 585 Purdue Mall, West Lafayette, IN 47907, USA.
c. Argonne National Laboratory, 9700 South Cass Avenue, Lemont, IL 60439, USA. Email: Luzhang@anl.gov.

To elucidate the electrochemical reactions and identify the redox pairs, cyclic voltammetry (CV) was used to investigate the redox properties of **TPz** redoxmers. Notably, the **TPz** molecules demonstrate a dissimilar redox behavior compared to the parent phenazine, **DHPS**. As shown in Figure 1a, **DHPS** exhibits a concerted 2e$^-$ reaction in an alkaline electrolyte (*i.e.*, 1 M NaOH), forming a dianionic reduced state and involving no radical species. The separation between the reduction and oxidation peaks is 402 mV, which agrees well with our previous result.[11] In contrast, **TPz** molecules show stepwise redox events in the same alkaline electrolyte, e.g., at -0.64 V and -0.96 V vs Ag/AgCl in the case of **TPz-2**. This phenomenon is also observed for **TPz-1**, indicating its independence of substituents. The peak separations of the two redox events in both **TPz-1** and **TPz-2** are in a range of 30 to 40 mV, indicating more than one transferred electrons involved in each step (1e$^-$ corresponding to 59 mV). Based on the CV results, it is speculated that **TPz** redoxmers undergo two-step redox reactions (Scheme 2a). In the tripod structure of **TPz**, each "pod" bears a phenazine unit that is responsible for the redox activity. In the charging process, **TPz** receives an electron at each pod, yielding an overall of three radical anions in the core that is conjugative to a radical anion intermediate **TPz$^{\bullet 3-}$** (Step 1). Then, in the second step, the **TPz$^{\bullet 3-}$** gains three additional electrons to form the hexa-anion species **TPz^{6-}**. The discharging process follows the reversed stepwise reactions, *i.e.*, from **TPz^{6-}** to **TPz$^{\bullet 3-}$** then to **TPz** via successive loss of three electrons. This argument is further supported experimentally by the following **TPz**-based flow cell test results.

The electrochemical kinetic characteristics of **TPz** molecules were evaluated based on the CV curves collected at different scan rates, using a reported method.[16] The detailed procedure is described in Section S3 in the ESI. Assuming three transferred electrons in each of the two steps, the diffusion coefficients (D) of **TPz-2** are 3.16×10^{-8} cm^{2}s^{-1} for the first and 8.88×10^{-8} cm^{2}s^{-1} for the second redox couples, respectively. The diffusion rates of **TPz-2** species are about two orders of magnitude lower than that of **DHPS** ($D = 3.39 \times 10^{-6}$ cm^{2}s^{-1}), primarily due to its significantly larger molecular size. In addition, because of the extensive conjugation in **TPz-2**, a second possibility for the slow
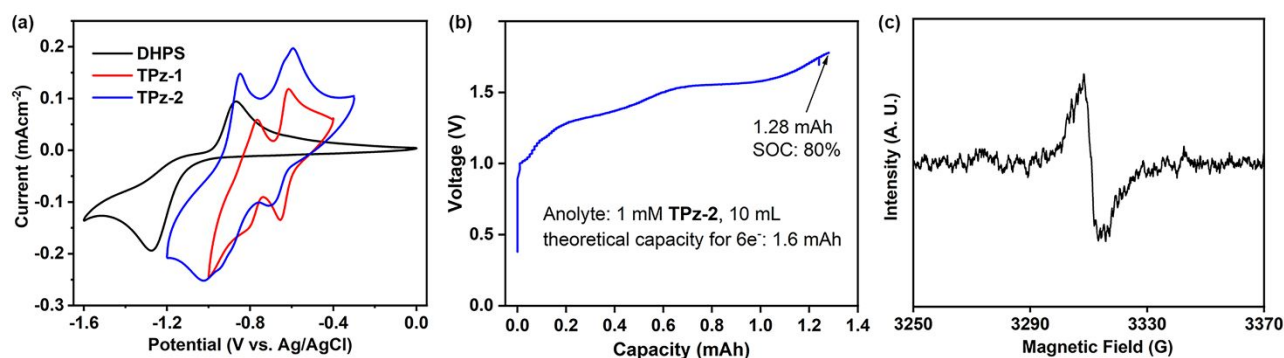

Figure 1. (a) CV curves of 3 mM **TPz-1**, **TPz-2** and **DHPS** in 1.0 M NaOH at 100 mVs^{-1}; (b) a charging voltage curve of a 1 mM **TPz-2** flow cell at 3 mAcm^{-2}; (c) First derivative absorption EPR spectrum of electrochemically prepared 1 mM **TPz-1$^{\bullet 3-}$**.

diffusivity is its π-stacking to the graphitic surface of the glassy carbon electrode used in CV tests, leading to slow interfacial adsorption and desorption. The electrochemical rate constants (k_0) of **TPz-2** are 1.13×10^{-5} cms^{-1} and 1.69×10^{-5} cms^{-1} for the first and the second redox reactions, respectively, which are comparable to that of **DHPS** (1.01×10^{-5} cms^{-1}) and other phenazine based redoxmers[17].

The electrochemical performance of **TPz-2** as the anolyte redoxmer was evaluated in an alkaline aqueous redox flow battery. The Fe(CN)$_6^{4-}$/Fe(CN)$_6^{3-}$ catholyte couple has been widely used to evaluate anolyte molecules in alkaline electrolytes because of its acceptable stability,[10, 18] and thus was used in our work. It has a redox potential of 0.34 V vs Ag/AgCl. Thus, the flow cell achieves cell voltages of 0.98 V and 1.30 V, respectively, for the first and second redox couples of **TPz-2**. Although **TPz-2** has a decent solubility of 0.3 M, its fully charged species suffer from low solubility. A solid precipitate was observed when the flow cell using 0.05 M **TPz-2** was charged. This is presumably because the ultra-high electron density enables strong **TPz-2^{6-}**-Na$^+$ ion pairing forces that prevail over the **TPz-2^{6-}**-water solvation interactions.[19] Therefore, much

lower **TPz-2** concentrations were used to demonstrate the multi-electron activity in flow cells.

Figure 1b shows the charging voltage curve of a flow cell using 1 mM **TPz-2** anolyte in 1 M NaOH. The catholyte was used in excess (0.06 M) to avoid complication by its relative instability in alkaline electrolytes[20] and make anolyte as the limiting side. Two voltage plateaus are clearly visible at approximately 1.35 V and 1.55 V, respectively. Each plateau contributes near-equally to the overall charged capacity of 1.28 mAh that corresponds to 80% of the theoretical capacity (1.6 mAh) for 6e$^-$ redox. Moreover, in our initial flow cell test using 1 mM **TPZ-1**, when the charging was limited to the first 3e$^-$, an electron paramagnetic resonance (EPR) signal was captured in a sample aliquot extracted from the anolyte (Figure 1c), indicating the existence of a radical species, most likely **TPz-1$^{\bullet 3-}$**, at this charged stage. These observations corroborate the CV results to provide robust evidence that validates the proposed 6e$^-$ redox activity and stepwise redox mechanism for **TPz** redoxmers. It is worth mentioning that a previous hybrid RFB using **TPz** as a non-flow anode also suggested a six-electron redox activity, providing a reported mechanism for **TPz** redoxmers. It is worth mentioning that a precedent that supports our argument.[21]

Journal Name

COMMUNICATION

The rate capability of a flow cell using 5 mM **TPz-2** is plotted in Figure 2a. As the current density increases from 3 to 15 $mAcm^{-2}$, the coulombic efficiency (CE) slightly increases from 97% to near-100% but the voltage efficiency (VE) drops significantly from 84% to 48%. Consequently, the energy efficiency (EE) drops from 81% to 48%. In general, the flow cell needs to be operated at relatively low current densities to achieve good efficiencies. Such a rate performance is rather

inferior compared to the **DHPS** based flow cell (Figure S9 in the ESI). A previous report also shows that **DHPS**-based flow cells achieved >90% EE even at a current density of 50 $mAcm^{-2}$.[11] To understand the different rate behaviors, electrochemical impedance spectroscopy (EIS) measurement was performed to **TPz-2** and **DHPS** flow cells under the same conditions. Based on their Nyquist plots (Figure 2b), while the two flow cells have very similar area-specific ohmic (R_Ω) and charge transfer (R_{CT})
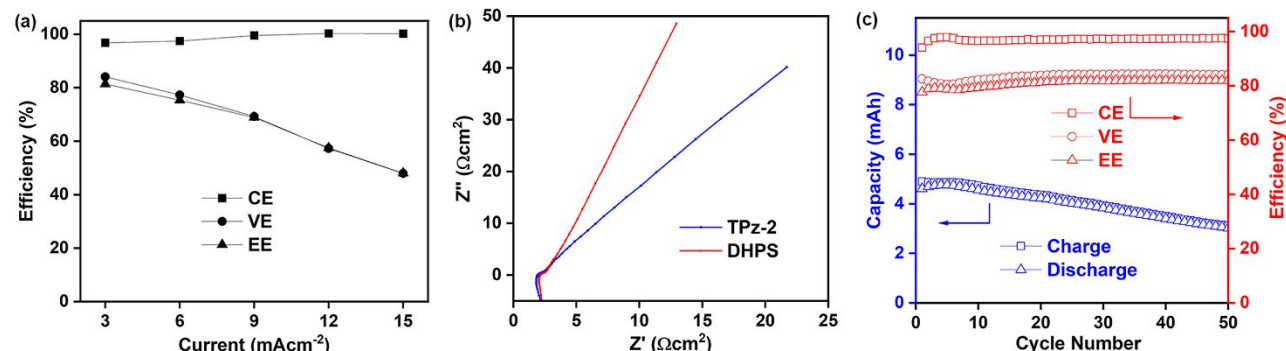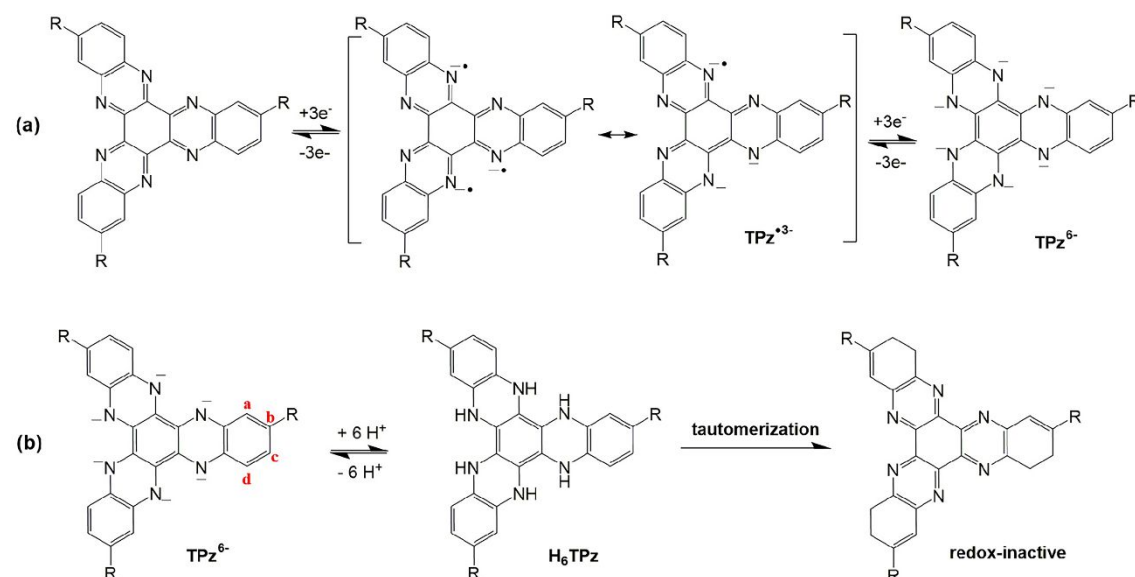

Figure 2. (a) Rate capability of 5 mM **TPz-2** flow cell; (b) Nyquist plots of **TPz-2** and **DHPS** flow cells under the same conditions; (c) cycling efficiency and capacity of 5 mM **TPz-2** flow cell at 3 $mAcm^{-2}$.

Scheme 2. (a) The proposed stepwise redox mechanism of **TPz** redoxmers; (b) the possible decomposition pathway of fully charged **TPz** redoxmers (**TPz⁶⁻**) via tautomerization.

resistances, the **TPz-2** flow cell shows a significantly higher Warburg (or diffusion) resistance (W) indicated by the smaller slope of the straight line in the low-frequency region. The EIS result agrees well with the comparable k_0 but contrastive D for **TPz-2** and **DHPS** obtained from CV tests. Thus, it appears to us that the inferior rate performance of **TPz-2** flow cell may originate from its much lower diffusivity that is expected to result in longer adsorption/desorption time scales. This is somewhat counter-intuitive as the electrolyte circulation usually facilitates mass transport. But if this argument is the case, this phenomenon will pose a critical challenge for large-size redoxmers such as **TPz** to produce good RFB efficiency, to

which a solution must be developed to achieve improved RFB performance.

To evaluate the cycling stability, a 5 mM **TPZ-2** flow cell was galvanostatically tested at a constant current of 3 $mAcm^{-2}$. The efficiency and capacity are outlined in Figure 2c. One cycle corresponds to approximately 20 minutes. No solid precipitate was observed in the anolyte solution. The flow cell demonstrates an average CE of 97%, VE of 84% and EE of 81%. The cycling capacity corresponds to ~60% of the theoretical 6e⁻ capacity in the initial cycles. However, a gradual capacity fading at an average rate of 0.6% per cycle (*i.e.*, 55% per day) is detected. As shown in Figure S10 in the ESI, a fully charged **TPz-2** flow cell exhibited a gradual voltage drop when standing idle.

COMMUNICATION

According to the prior studies of phenazine-based redoxmers,[22, 23] the most possible cause for the capacity fading is decomposition of **TPz** redoxmers especially in the charged states. The siting of substituent groups plays a critical role in controlling the chemical stability of charged phenazine species. With substituents at *b-* and *c*-positions of **TPz-2**, chemical decomposition via a tautomerization pathway to form redox-inactive side products is highly possible (Scheme 2b). Moving the substituents to *a-* and/or *d*-positions may yield improved chemical durability and cycling stability in flow cells. Inspired by these findings, synthesis and evaluation of more stable **TPz** derivatives are our ongoing efforts. Another possible factor for the degradation may be the unwanted interactions between organic redoxmer and Nafion membrane that lead to enhanced cell resistance. Such a phenomenon has been commonly observed in ion exchange membrane-based flow cell tests.[11]

Conclusions

In summary, we have successfully developed a novel organic anolyte redoxmer structure that affords six transferred electrons in the context of redox flow batteries. The molecular design bearing redox-active macroaromatic **TPz** scaffold and solubilizing substituents has been demonstrated effective to enable six-electron redox activity with decent solubility. Moreover, the fused tripod core of **TPz** exhibits a drastically different stepwise redox mechanism yet similar redox kinetics compared to the parent phenazine (**DHPS**). Among the synthetic **TPz** molecules, **TPz-2** exhibits an enhanced solubility of 0.3 M and two redox events at -0.64 V and -0.94 V vs Ag/AgCl in pH 14 electrolyte. The low-concentration flow cells using **TPz-2** anolyte and ferri/ferrocyanide catholyte successfully demonstrates a six-electron redox capability but meanwhile shows relatively low efficiency and relatively fast capacity drop. As the major challenge, our current **TPz** flow cell testing has no practical relevance because of the extremely low tested concentration and current density. To make this family of redoxmer structures attractive, further optimization efforts are ongoing focused on tailoring the hydrophilic moiety, number, and siting of substituents on the **TPz** redox center to achieve synergistic property improvement. Nevertheless, our preliminary results demonstrate an under-developed but promising multi-electron molecular design strategy for the development of energy-dense redox flow batteries.

1. G. L. Soloveichik, *Chem Rev*, 2015, **115**, 11533-11558.
2. W. Wang, Q. T. Luo, B. Li, X. L. Wei, L. Y. Li and Z. G. Yang, *Adv Funct Mater*, 2013, **23**, 970-986.
3. C. Ding, H. M. Zhang, X. F. Li, T. Liu and F. Xing, *J Phys Chem Lett*, 2013, **4**, 1281-1294.
4. Y. Ding, C. K. Zhang, L. Y. Zhang, Y. E. Zhou and G. H. Yu, *Chem Soc Rev*, 2018, **47**, 69-103.
5. J. Luo, B. Hu, M. Hu, Y. Zhao and T. L. Liu, *Acs Energy Lett*, 2019, **4**, 2220-2240.
6. T. B. Liu, X. L. Wei, Z. M. Nie, V. Sprenkle and W. Wang, *Adv Energy Mater*, 2016, **6**, 1501449.
7. Y. H. Liu, M. A. Goulet, L. C. Tong, Y. Z. Liu, Y. L. Ji, L. Wu, R. G. Gordon, M. J. Aziz, Z. J. Yang and T. W. Xu, *Chem-Us*, 2019, **5**, 1861-1870.
8. X. Fang, Z. Li, Y. Zhao, D. Yue, L. Zhang and X. Wei, *ACS Materials Letters*, 2022, **4**, 277-306.
9. B. Huskinson, M. P. Marshak, C. Suh, S. Er, M. R. Gerhardt, C. J. Galvin, X. D. Chen, A. Aspuru-Guzik, R. G. Gordon and M. J. Aziz, *Nature*, 2014, **505**, 195-198.
10. K. X. Lin, Q. Chen, M. R. Gerhardt, L. C. Tong, S. B. Kim, L. Eisenach, A. W. Valle, D. Hardee, R. G. Gordon, M. J. Aziz and M. P. Marshak, *Science*, 2015, **349**, 1529-1532.
11. A. Hollas, X. L. Wei, V. Murugesan, Z. M. Nie, B. Li, D. Reed, J. Liu, V. Sprenkle and W. Wang, *Nature Energy*, 2018, **3**, 508-514.
12. C. Wang, X. Li, B. Yu, Y. Wang, Z. Yang, H. Wang, H. Lin, J. Ma, G. Li and Z. Jin, *Acs Energy Lett*, 2020, **5**, 411-417.
13. C. Zhang, Z. Niu, S. Peng, Y. Ding, L. Zhang, X. Guo, Y. Zhao and G. Yu, *Adv Mater*, 2019, **31**, 1901052.
14. P. W. Antoni, C. Golz and M. M. Hansmann, *Angewandte Chemie International Edition*, 2022, e202203064.
15. J. H. Huang, S. Z. Hu, X. Z. Yuan, Z. P. Xiang, M. B. Huang, K. Wan, J. H. Piao, Z. Y. Fu and Z. X. Liang, *Angew Chem Int Edit*, 2021, **60**, 20921-20925.
16. H. Wang, S. Y. Sayed, E. J. Luber, B. C. Olsen, S. M. Shirurkar, S. Venkatakrishnan, U. M. Tefashe, A. K. Farquhar, E. S. Smotkin, R. L. McCreery and J. M. Buriak, *Acs Nano*, 2020, **14**, 2575-2584.
17. J. C. Xu, S. Pang, X. Y. Wang, P. Wang and Y. L. Ji, *Joule*, 2021, **5**, 2437-2449.
18. R. Feng, X. Zhang, V. Murugesan, A. Hollas, Y. Chen, Y. Shao, E. Walter, N. P. Wellala, L. Yan and K. M. Rosso, *Science*, 2021, **372**, 836-840.
19. M. O. Hurst and R. C. Fortenberry, *Comput Theor Chem*, 2015, **1069**, 132-137.
20. J. Luo, A. Sam, B. Hu, C. DeBruler, X. L. Wei, W. Wang and T. L. Liu, *Nano Energy*, 2017, **42**, 215-221.
21. Z. R. Liu, Z. Wang, Y. J. Shi, Y. M. Shen, W. C. Wang, Z. D. Chen, J. Xu and J. Y. Cao, *J Mater Chem A*, 2021, **9**, 27028-27033.
22. N. P. Wellala, A. Hollas, K. Duanmu, V. Murugesan, X. Zhang, R. Feng, Y. Shao and W. Wang, *J Mater Chem A*, 2021, **9**, 21918-21928.
23. S. Pang, X. Wang, P. Wang and Y. Ji, *Angewandte Chemie International Edition*, 2021, **60**, 5289-5298.

Conflicts of interest

There are no conflicts to declare.